Phase stable RF cable for space applications

Space Passive Component Days, 1st International Symposium

H. Karstensen[1], I. Koufogiannis [2], E. Sorolla[2], G. Kress[3], M. Mattes [2], M. Rupflin[1], J. Fuchs [1], K. Wettstein[1]

[1] *HUBER+SUHNER AG*
Degersheimerstr. 14, CH-9100 Herisau (Switzerland)
Email: holger.karstensen@hubersuhner.com
[2] *Ecole Polytechnique Federal Lausanne*
PO Box Station 11, CH-1015 Lausanne (Switzerland)
Email: michael.mattes@epfl.ch
[3] *Eidgenössische Technische Hochschule Zurich*
Leonhardstr. 27, LEO C2, CH-8092 Zürich (Switzerland)
Email: gkress@ethz.ch

ABSTRACT

Within the ESA contract 22589 we have designed and are currently fabricating cable assemblies based on a completely novel approach with incorporating an InVar made inner conductor (extremely low thermal expansion) and a non-homogeneous dielectric, the so-called SucoPearl approach. This is an insulation consisting of a large number of individual pieces of dielectric material that are threaded along the inner conductor, like pearls on a chain.
The goals of the design are prioritized as follows:
1. High phase stability, low loss
2. Low mass
3. High power.

Generally, the proposed design is – in terms of phase stability and low loss requirements - close to the physical limit of the chosen cable dimensions, resulting in an extremely light-weight cable. A few performance requirements (maximum power handling being the most important) had to be adapted in order to achieve best performances for the prioritized high phase stability.
All processes and materials are chosen to be space compliant. Moreover, all manufacturing processes are designed for low cost production although the fabrication techniques for the design of certain coaxial cables differ completely from the conventional ones.
Mechanical forces, pressures on the dielectric introduced by the tape and the stranding of the outer conductors are taken into account as well as the displacement of the inner conductor due to bending of the cable and to lateral pressure.
Venting has been simulated (and verified by first measurements of early prototypes) by setting up a venting model for this type of cable that simulates the pressure inside the vacuum chamber and the cable over time.
Early prototypes have already been manufactured and showed excellent phase stability and high power handling capabilities, while the second prototype generation is currently in fabrication.

INTRODUCTION

Presently, lightweight RF power cables show serious drawbacks due to the poor heat evacuation from the inner conductor to the outside environment of the cable and due to their poor phase stability. The last one is an extremely important requirement when combining amplifiers in reconfigurable or extremely high power payloads. For future telecom payloads, new generation of ultra-light RF cables capable of handling high RF power signals with high phase stability are required. Alternatively, the use of Medium Power Amplifiers (MPA) is prohibitive as a large number of cable assemblies is necessary, implying a significant mass increase. Consequently, new cables need to be lightened in the order of 30-40% and also meet more severe requirements on phase stability as compared to currently available products without degrading any other RF parameter.
The new cable sizes will be compatible with the currently produced HUBER+SUHNER cables SUCOFLEX304 (SF304) and SUCOFLEX306 (SF306), flexible cables with 4 mm and 6mm, inner diameter of the outer conductor, respectively. The connectors assembly intended to work with the new designs will be either the TNC or the new PSM connector, depending on the cable size.

So far, one type of cable has been completely designed, simulated and fabricated: the SP304_FEP. The cable size corresponds to the HUBER+SUHNER type SUCOFLEX304, so that cable connectors for space operation are already available or can be adapted to the new cable entries with moderate effort.

Additionally to the SP304_FEP provided with an outer diameter of 5.38 mm, very low mass and a high cut-off frequency (greater than 26.5 GHz), another design, the SP306_FEP, is planned with an outer diameter of 7.55 mm, slightly increased mass (around 100 g/m) but with lower attenuation and a cut-off frequency of 20 GHz.

The SP304_FEP comes with an Ag-plated InVar inner conductor, a dielectric made of PTFE pearls, an FEP inner jacket, and an Ag-plated Cu band plus a Cu/Ag-plated Al braid. The mass is 46.4 g/m and the cut-off frequency 29.4 GHz. At 18 GHz the loss is 0.9 dB/m whereas it remains bounded below 1.1 dB/m. The additional FEP inner jacket causes here a slight, but still acceptable, increase of the insertion loss.

Both cables show a phase change less than 500 ppm within the temperature range lying from -55°C to 200°C.

The major difference with respect to standard cables is the kind of dielectric that here it consists of a large number of hollow parts ("pearls"). A big advantage of this approach is the fact that the inner conductor and the dielectric can be designed and fabricated independently, thus giving the chance to optimize the characteristics individually.

TECHNICAL APPROACH
SucoPearl with inner jacket
As manufacturing difficulties with the taping process due to the varying outer diameter can occur it has been proposed to add a relatively stiff extruded layer directly on top of the pearls (inner jacket). This layer can be made out of FEP. This material has good mechanical properties although it will contribute considerably to the cable loss (tanδ=0.0006, >6x that of PTFE). This layer therefore has to be made as thin as possible but without compromising the mechanical stability of the cable.

The design will look like that one shown in Fig. 1 (cable SP306_FEP, sizes like SF106).
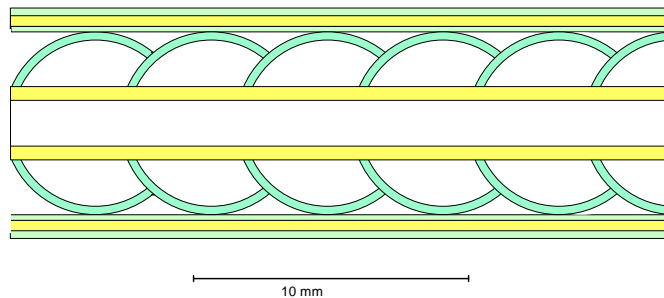

10 mm

Fig. 1: Design of the SP304_FEP cable with inner jacket.

Modeling and Simulation
The preferred cable sizes are those that correspond to the HUBER+SUHNER types SF304 and SF306. They are named SP304_FEP and SP306_FEP. One of the reasons for this amongst others is their suitability to work with the connectors that are already available in the market for space operation.

Whereas the SP304_FEP, with an outer diameter of 5.38 mm, shows low mass and a high cut-off frequency, the SP306_FEP, with an outer diameter of 7.55 mm, has much more mass (around 100 g/m) but less attenuation and a cut-off frequency of 20 GHz.

The details will be presented in the following sections.

SP304_FEP
The SP304_FEP cable has a Ag plated inner conductor, a dielectric made of PTFE pearls, an FEP inner jacket, and a Ag-plated Cu band plus a Cu/Ag-plated Al braid.

The mass is 46.4 g/m, the cut-off frequency 29.4 GHz. The simulated S-parameters are shown in Fig. 4 and Fig. 5. At 18 GHz the loss is 0.9 dB/m, at 26.5 GHz still 1.1 dB/m. The additional FEP inner jacket causes here a slight increase of the insertion loss.
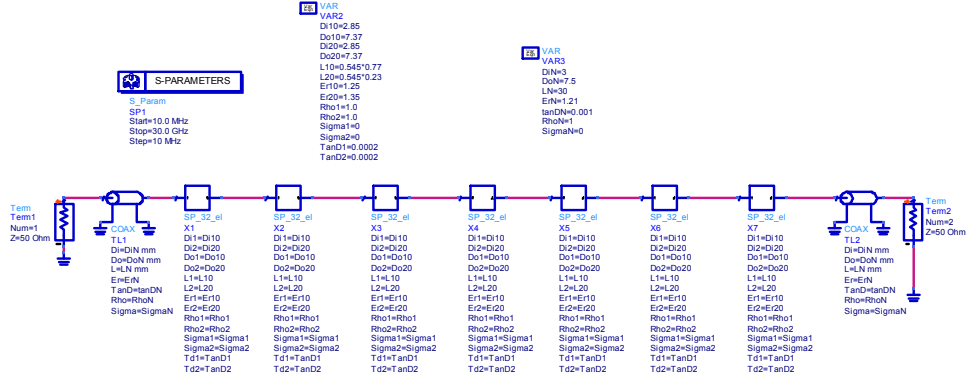
Fig. 2: S-Parameter Model of SucoPearl (60 cm long)

The SucoPearl cable has been simulated with the model shown in Fig. 2. It consists of 7 subcircuits of 16 pearls that is shown in Fig. 3. So the total number of pearls is 112, corresponding to a cable length of 112 times the length of a period L_p=5.35 mm, i.e. 59.92 cm.
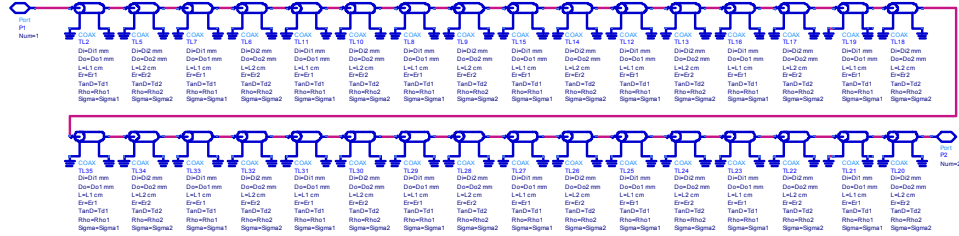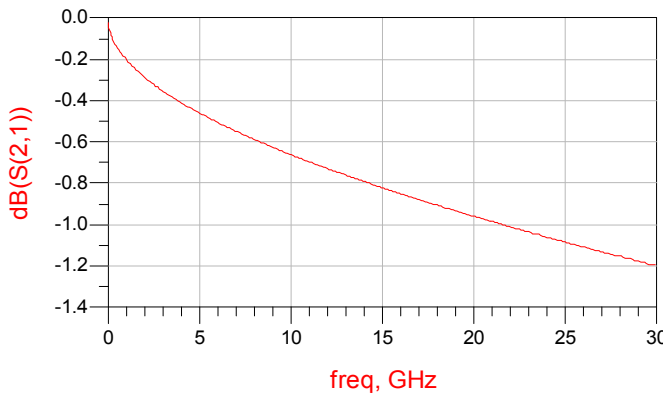

Fig. 3: Subcircuit for 16 Pearls

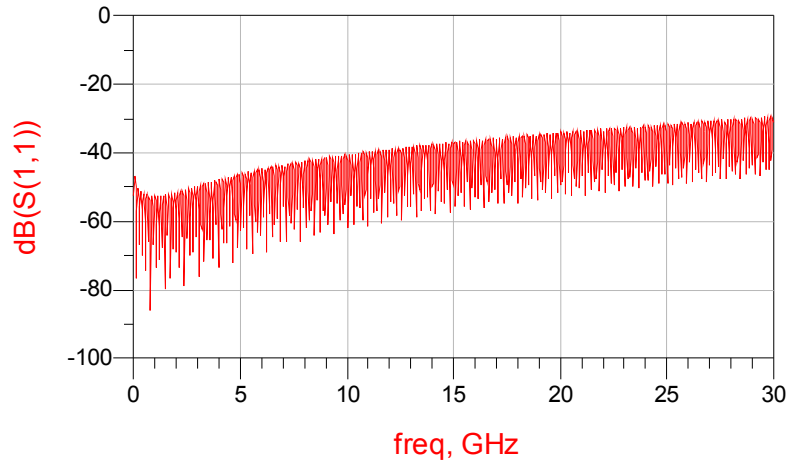**Fig. 4: Simulated insertion loss or the SP304_FEP cable (length 1m)**

Fig. 5: Simulated reflection loss of the SP304_FEP cable (length 1m)

SucoPearl Design Coaxial Cable Bending Behavior
SucoPearl Parameters and Spacing
The thickness of a SucoPearl's wall is assumed constant over its whole spherical region. The parameters include the opening angle φ which decides over the periodic length and radius of contact with the adjacent SucoPearl, the inner and outer radii of the sphere, and the radius of the inner conductor which is assumed to be the same as the radius of the corresponding SucoPearl hole.
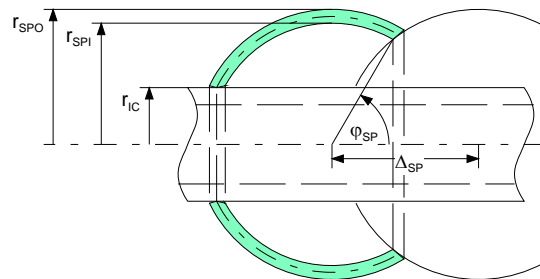

Fig. 6: SucoPearl Geometry parameters

Bending Kinematics
Influence of relative stiffness of inner and outer conductors and SucoPearls
Assumptions on the relative stiffness of the structural components of the coaxial cable lead to simplifications on which closed-form analytical models for estimating the eccentricities induced by bending can be based. We suggest three different assumptions and outline their consequences on bending behavior:
1. The SucoPearls are much less stiff than the other components
2. The inner conductor is much less stiff than the other components
3. The outer conductor is much less stiff than the other components:

The current cable design features an inner conductor which is a solid tube made of IinVar steel while the outer conductor is made of a helically wound copper band. The outer conductor is covered with a shield made from aluminum weave. Both of these components are much less stiff in extension as well as bending than the inner conductor. This design has been chosen to allow for relatively small bending radii as large material strains will be induced only in the inner conductor whose radius is relatively small if compared to that of the cable. Therefore, the third of the above assumptions agrees best, and actually quite well, with the current cable design.

The smaller hole of a SucoPearl fits the inner conductor diameter but it is assumed that the SucoPearl can rotate about the center of the smaller hole. This requires deformation of the SucoPearls in the region of the small hole and contradicts the notion of rigid-body kinematics. The error will become as small as possible, if the contour along the inner hole is designed as indicated in Fig. 6. Results indicate that the strains in the SucoPearls caused by the rotation are small enough to be sustained without damage.

The larger hole forms circular edges with the inner and the outer SucoPearl surfaces. One of these can be in gapless contact with the outer surface of the adjacent SucoPearls, respectively. It has been chosen here that the edge at the inner surface will be in contact. The risk of any gaps to appear is minimized if the surface between the both edges is tangential to the other's SucoPearl's surface, which design is indicated by Fig. 6.

Model derivation

The center line of the inner conductor is bent to a circle with nominal radius R_N. The center points C of the small holes of the SucoPearls are on that circle. If the SucoPearls have a spherical shape, sliding of the edge of the large hole of one pearl on the spherical surface of the adjacent pearl, so that no gap between the edge and the surface occurs, is possible if the pearl with edge rotates about the center point A of the other pearl as Fig. 7 illustrates. The same figure shows that the gapless sliding of a SucoPearl (green or blue) on the surface of an adjacent SucoPearl (grey) is the same as a rotation of the sliding pearl about the center point of adjacent pearl, and therefore the points A, B, and C are always connected by a straight line.
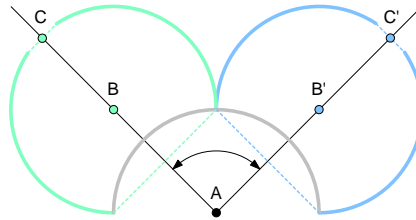

Fig. 7: Sliding of a SucoPearl (colored) on its adjacent neighbor (grey)

Because of the periodicity of the system, both sphere centers, A and B, must lie on the same radius R_{CP}, which is smaller than R_N as Fig. 8 illustrates. As the outer conductor's and the sphere's center lines must be identical, the eccentricity is given by the difference of the values of the radii R_N and R_{CP}.
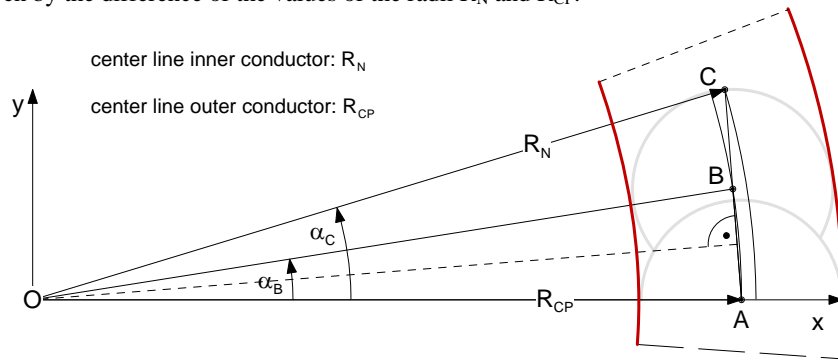

center line inner conductor: R_N

center line outer conductor: R_{CP}

Fig. 8: The sphere centers lie on a smaller radius than the inner conductor center line

Comparison with results by a model after the Finite-Element Method

Numerical simulations by using the Finite-Element Method (FEM) have been performed and the predictions compared to the present analytical model. The finite-element modeling takes advantage of the periodicity of the cable structure as Fig. 9 indicates.
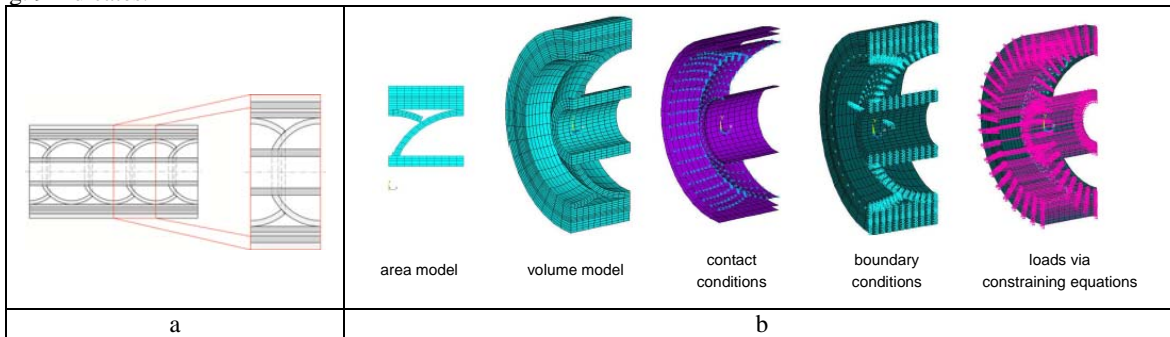

a	b
	area model · volume model · contact conditions · boundary conditions · loads via constraining equations

Fig. 9: Geometric unit cell of the periodic cable structure and FEM modelling steps

The unit-cell model is established by algorithms programmed into a data generator which reads in a small number of model parameter data and writes to a text file the much larger data set defining the geometric entities, the finite-element mesh, the contact conditions between model parts, the boundary conditions, and the inhomogeneous constraining equations describing the periodicity of deformations as well as the defined amount of bending. The data shown in Table 1 suggest that the eccentricities, predicted by both models, deviate from each other by less than 3 %.

Table 1: Comparison of results for SP304_FEP

Opening angle [°]	Eccentricity [microns] Numerical model	Eccentricity [microns] Kinematical model	Difference in [%]
50	68.0	70.0	2.9
55	65.4	66.6	1.7
60	62.3	63.0	1.0
65	58.7	59.4	1.2

Results

The opening angle φ determines the end of the sphere, with it the length of one SucoPearl, and the size of the opening with which it contacts the neighboring SucoPearl. These geometric properties have an influence on the periodicity spacing, the minimum bending radius which must not be smaller if a given eccentricity must not be exceeded, and the material volume per unit length.

This design gives a good protection against the occurrence of direct viewing lines from the outer to the inner conductors. On the other hand, if the contacting ring slides on a sphere, there is no cause for any gaps between the contacting bodies to occur. Also, the design allows the opening angle to be as large as 90 degrees.

Fig. 10 provides insight into the nature of the optimization problem: the weight and the minimum bending radius give a conflict of objectives. One has to choose, or find a compromise, between high bending abilities (opening angle close to 90 degrees) or low weight (opening angle close to 150 degrees). The averaged strains are too small to be an issue. They will be easily digested by small elastic deformations and, in any case, they are negative which helps preventing gaps between contacting SucoPearls to occur.

Another optimization parameter concerns the shape of the SucoPearls. The ideas underlying the kinematical model are based on a spherical shape which seems to be ideal as it systematically does not lead to gaps. The parameters to be optimized include only the opening angle and the inner contour, or the wall thickness, of the SucoPearls.

It is in accordance with the kinematical assumptions that the SucoPearls should be placed on the inner conductor with a tight fit. On the other hand, the width of the SucoPearl's wall at that fit should be small enough to allow for the kinematically necessary rotation

The small holes of the SucoPearls have been assumed to have the same radius as that of the inner conductor. Rotation of the SucoPearls relative to the latter must then cause material deformation. The right most column in Table 2 gives the averaged strains which are all below one tenth of one percent. The values are small enough to not cause material failure.

The designs currently considered by Huber+Suhner specify an angle $\theta_1=51^\circ$ for the type SP304_FEP.

Results for SP304_FEP

Geometric data for this type are $R_{SPO}=1.93$mm, $R_{SPI}=1.73$mm, $R_{SPH}=r_2=0.815$mm. The minimum bending radii causing an eccentricity of 40 micrometers are listed in Table 2. They become smaller with increasing opening angles but the minimum possible bending radius cannot be smaller than 61.5mm. It is slightly more than ten times the cable diameter, or 53.8mm. The axial strain caused by the allowable bending decreases with decreasing opening angle. On the other hand, the material volume per unit length increases with increasing opening angle. Therefore, the solution with best bending capabilities is the one with the highest weight penalty.

Table 2: SP304 spacing of periodicity, minimum bending radius for eccentricity 40 micrometers, specific volume, and averaged axial strain

φ	$\Delta_{SP}[mm]$	$R_N^{\min}[mm]$	$v[mm^3/mm]$	$\bar{\varepsilon}_{axial}[\%]$	$\bar{\varepsilon}_{SPH}[\%]$
30	3.224	115.5	12.30	-0.0222	0.044
40	2.903	108.3	13.05	-0.0228	0.046
50	2.515	99.4	14.18	-0.0238	0.048
60	2.082	89.4	15.92	-0.0251	0.052
70	1.632	79.2	18.64	-0.0265	0.056
80	1.207	69.5	22.95	-0.0281	0.061
90	0.856	61.5	29.30	-0.0293	0.067

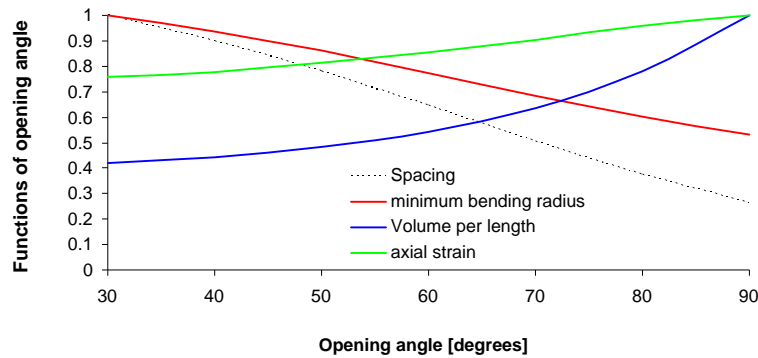Normalized values of the data listed in Table 2 are plotted in Fig. 10.

Fig. 10: Normalized Functions of opening angle for SP304

PHASE STABILITY ANALYSIS
One of the basic strengths of the proposed design is the very low phase shift when the cable is installed and operated in the hazardous space environment.
Two independent cases of phase shift stability are generally considered. When a cable is operating, then the change of the temperature due to ohmic losses and the ambient temperature results in a perturbation of the electrical and structural properties of the materials of the cable. This effect is noted as phase stability vs. temperature to be distinguished from the phase stability vs. bending. The latter is a result of the change of the characteristics of the propagating mode when the cable is bent.
Both phase stability issues are addressed in the following sections. With the phase $\varphi_0 = \varphi(T_0, f_0)$ at temperature T_0 and frequency f_0 we get for the relative phase change as function of the temperature the expression:

$$\frac{\Delta\varphi}{\varphi_0} = \frac{\varphi(T,f) - \varphi_0}{\varphi_0} = -\frac{t_d(T,f) - t_d(T_0,f_0)}{t_d(T_0,f_0)}$$

Frequency dependence of permittivity
To obtain the frequency dependence of the permittivity it is helpful to measure the difference $\Delta\varphi$ of the absolute phase $\varphi(f)$ at frequency f and the ideal phase $\varphi_0(f)$ with a constant phase velocity v_{phref}, where the reference phase velocity is the actual phase velocity at half maximum of the frequency range, e.g. $v_{phref} = v_{ph}(10GHz)$ when the measurement range is 20GHz.
The evaluation of the phase measurements of homogeneously filled cables revealed the permittivity of PTFE vs. frequency, the results is shown in Fig. 11.
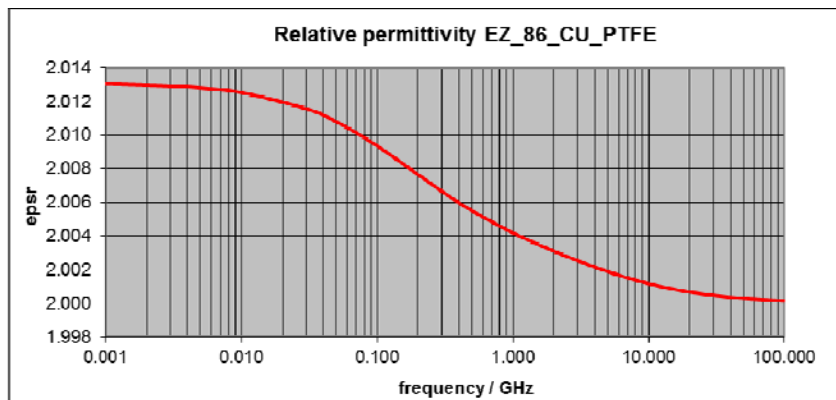

Fig. 11: Relative permittivity of the EZ86 cable with PTFE foam dielectric (from phase measurement data)

Temperature dependence of PTFE permittivity

For a given frequency f_0 the only parameters that change with temperature are the length L and the relative permittivity ε_r [1],[2],[3]. Hence we get for the phase change in dependence of temperature T and frequency f the relation:

$$\frac{\Delta\varphi}{\varphi_0}(T, f_0) = 1 - \frac{L(T) \cdot \sqrt{\varepsilon_r(T, f_0)}}{L(T_0) \cdot \sqrt{\varepsilon_r(T_0, f_0)}}.$$

The temperature dependence of the phase is measured for different frequencies. The results are shown in Fig. 12.
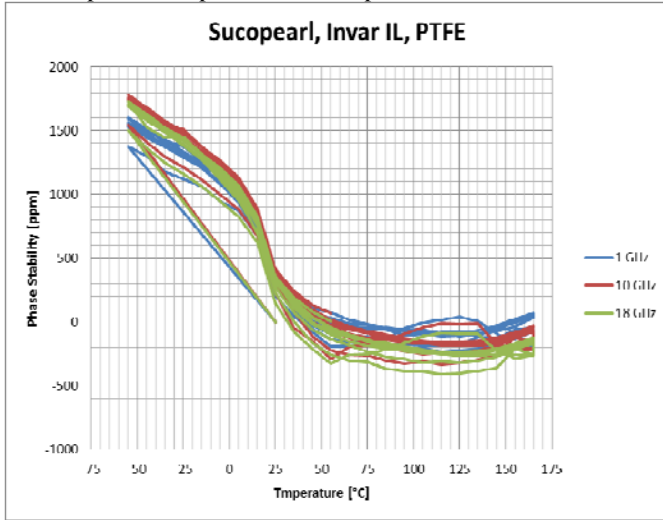

Fig. 12: Measured phase difference vs. temperature

A model that simulates the phase change as function of temperature and frequency has been developed. The simulated curves are shown in Fig. 13 for the SucoPearl cable with PTFE dielectric and an Invar-made inner conductor.
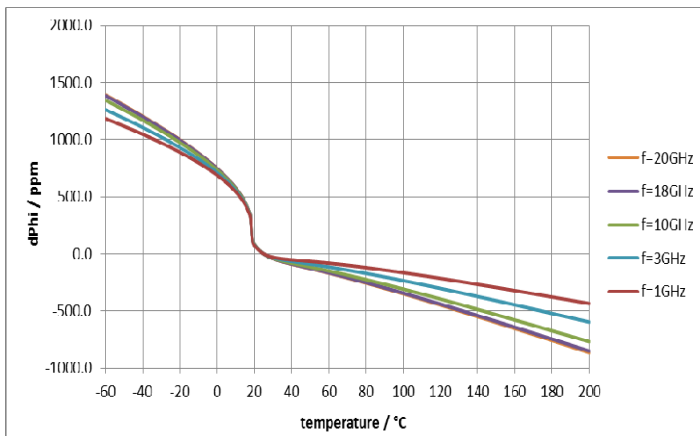

Fig. 13: Simulation of phase behaviour of SucoPearl with temperature and frequency dependent permittivity of PTFE

Measurements and simulations for the SucoPearl cable agree very well. Discrepances are believed to arise due to thermally induced mechanical changes of the outer conductor (braid in this case).

Eccentricity of the inner conductor

In case of a TEM mode, the propagation constant at high frequencies depends only on the medium impedance $Z_o = \sqrt{\dfrac{\mu}{\varepsilon}}$. Even if the inner conductor is moved and it is not any more centered, a TEM mode with exactly the same

propagation constant will be able to propagate. Only a change in the numerical values of the electric permittivity and permeability will be able to affect the propagation constant and consequently contribute to a change in the phase shift.
It is clear in the case of homogeneous cables, the electric permittivity and permeability are inherent values of the material that fills the space between the inner and outer conductor. In other words, the propagation constant of a TEM mode inside a homogeneous coaxial cable will not change if the position of the conductors varies.

Bending of the inner conductor
The propagation constant and the electric and magnetic field distribution of a TEM mode in a straight coaxial cable can be directly determined from the solution of the wave equation, assuming that the wave is propagating along a straight axis (commonly assigned as z-direction). If the propagation direction is not a straight vector but is tangential to a curvature with a fixed radius, then the usual solution of the TEM mode is not valid any more and the propagation constant and the tangential fields are perturbed. The perturbation in electric and magnetic fields of the TEM mode of a curved coaxial cable is of first order ($\propto 1/R$). Fortunately, the effect of bending in the propagation constant is only a second order phenomenon ($\propto 1/R^2$) [4]. However, as this project aims a product with very high phase stability, the second order term with respect to the radius is taken into account.
Then, considering the dimensions of the cable, the change in the propagation constant can be computed analytically and is plotted in Fig. 14 for different frequencies.
The phase stability vs. bending requirement involves a double loop with a radius equal to 85mm.
Under this configuration, the maximum perturbation in the propagation constant can be calculated through the following formula:

$$\frac{\beta}{k}\bigg|bend\_limit = \pm \frac{PSbend\_limit[\deg/GHz]*10^{-9}*c_o}{180*8*\pi*R_b[m]} + 1$$

where the PSbend_limit is given in the requirements, c_o is the speed of light in free space and R_b is the bending radius.
The perturbation in the propagation constant (colored lines) and the limits (dashed lines) coming from the specifications are also shown in Fig. 14 for different frequencies for the cable SP304.
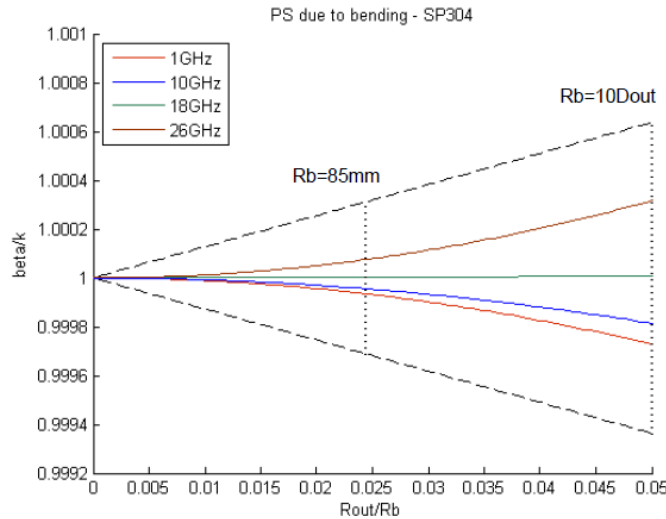

Fig. 14: Change in the propagation constant of SP304 for 1, 10 and 18GHz Dashed lines are the required limits and the dotted lines the maximum bending allowed (85mm or 10Dout).

In both figures the black solid line indicates the minimum bending radius proposed in the specifications. It is clear that both cables succeed in complying with the phase shift due to bending requirements for bending radius up to the electrical characteristics limit (R_b=85mm) and up to the mechanical characteristics limit (R_b=10D_{out}).

Multipaction Analysis of Sucopearl

In Fig. 15 the gaps of the cable SucoPearl where multipactor can occur are shown for a slice of the cable for the sake of visibility. As no software capable of dealing with boundaries made of different materials is available in the market, the material with the SEY whose first cross-over point is minimal has been chosen to avoid overestimating the multipactor withstanding capabilities of the cable. In this case, Silver has been considered in the simulations of multipactor since the first cross-over point of this material is lower than the one of PTFE or many other dielectrics.

As it can be seen in Table 3 the most critical gap of SucoPearl is the no. 3 with a threshold of 122 W at 1GHz, since its dimensions are close to the minimum of the multipactor susceptibility chart for Silver, and the gap starts in the inner conductor, where the electric field is maximal. The heights of gaps 4 and 5 are also close to the minimum of the Multipaction chart but the voltages along these gaps are lower. In the case of gap 4 the fringing field due to the presence of the dielectric is the responsible of this decrease of voltage, in the case of gap 5 the decrease is obvious since it lies far from the inner conductor. This threshold proves the excellent performance of SucoPearl regarding its multipactor withstanding capabilities, since this input power for space applications is a challenge for such a small cable.
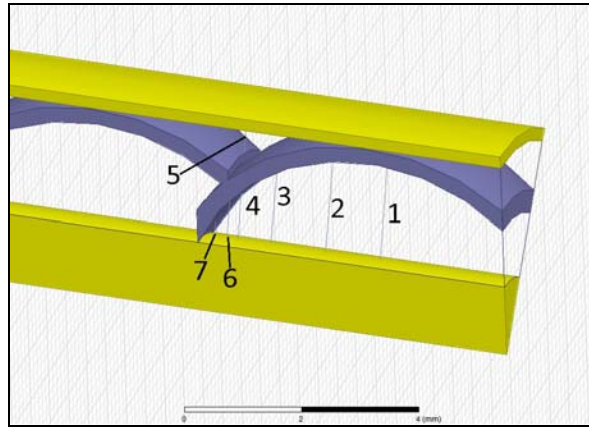

Fig. 15: Scheme of the gaps of the Sucopearl. The inner and the outer conductors are Silver-plated.

Table 3: Comparison of characteristics of different cable types

	Gap 1	Gap 2	Gap 3	Gap 4	Gap 5	Gap 6	Gap 7
Gap height (mm)	2.03	1.77	1.2	1.13	0.865	0.63	0.273
f (GHz)	**Breakdown power (W)**						
1	240	191	122	173	739	491	NO MP
4	4007	3892	2919	4421	$>10^4$	2378	1171
10	$>10^4$	$>10^4$	$>10^4$	$>10^4$	$>10^4$	$>10^4$	$>10^4$

Corona Analysis of Sucopearl

In order to calculate the Corona breakdown power threshold an in-house 2D FEM simulation tool has been implemented by reading the electric field from HFSS as input for the corona equation. Solving the eigenvalue problem of the matrix of the discretized corona equation for each pressure, the Paschen curve was found.

The plane where the corona equation has been solved was taken along the direction of the EM wave propagation as there is azimuthal symmetry (see Fig. 16). The maximum withstanding power without exhibting corona breakdown (P_B) isfound to be 51W occurring at a pressure of 1.9 mBars, as shown in Table 3. This shows the excellent high power withstanding capabilitites of Sucopearl, since this input power constitutes a challenge for coaxial cables of such small dimensions.
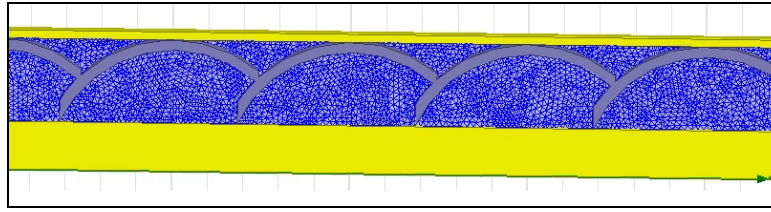
Fig. 16: Corona mesh layout of the SucoPearl cable.

Table 4. Corona breakdown threshold of SucoPearl.

Threshold @ 1 GHz	P_B (W)	P (mBar)
Sucopearl	51	1.9

MASS OF CABLES AND COMPARISON WITH STATE-OF-THE-ART CABLES

In Table 5 some characteristics of the proposed cables and a few other state-of-the-art cables are listed. The mass is lowest for the proposed SP304_FEP cable and the low-mass SF304 space cable. In both cases aluminum is used for the braid of the outer conductor, the SF304 also uses silver plated aluminum for the inner conductor. This is the reason for the large phase change with temperature.

In terms of phase stability, loss and low mass the newly proposed cables SP304_FEP and SP306_FEP are by far the best. The show lowest values for the phase change, for the mass and for the loss figures.

Table 5: Comparison of characteristics of different cable types

Cable type	temperature range	frequency range	phase change with temperature	phase change with bending	insertion loss	insertion loss	insertion loss	insertion loss	mass	max. power	Remarks
			-55°C - 125 °C	2 x 360°, 85mm	5.5 GHz	12 GHz	18 GHz	26.5 GHz		18 GHz, space	
		GHz	ppm	deg/GHz	dB/m	dB/m	dB/m	dB/m	g/m	W	
HS SP304_FEP	-55°C - 165°C	26.5	<400	±0.15	0.50	0.72	0.90	1.1	46	50	corona limit ?
HS SP306_FEP	-55°C - 165°C	18	<400	±0.2	0.33	0.50	0.65	---	80	>50	corona limit ?
HS SF304	-55°C - 150°C	18	<1500		0.66	1.16	1.44	--	46	50	thermal limitation
HS SF307	-55°C - 150°C	5.5	<1800		0.45		--	--	133	>200	thermal limitation
HS SF404	-55°C - 125°C	26.5	<1000	<1.5	0.50	0.75	1.00	1.15	66	150	thermal limitation
Ezforms EZ250	-65°C - 165°C	18	1800		0.66	1.14	1.45	--	125	75	
Ezforms EZflex401	-65°C - 200°C	18	1800		0.58	1.06	1.36	--	115		
Teledyne Reynolds 190E Phase Master	-55°C - 125°C	26.5	<800		0.64	0.95	1.18	--	69		
Times SiO2 0.270	-273°C - >200°	18	600		0.53	0.79	1.08	--	112		

CONCLUSIONS

It is shown that with the SucoPearl approach highly phase stable cables with a multipactor threshold >120 W at 1GHz and a corona threshold >50 W at the most unfavorable pressures between 1 and 2 mbar can be fabricated. The characteristics of the inner conductor, the dielectric and the outer conductor have to be tailored so that the temperature and bending induced effects compensate as good as possible.

The measured phase curve of the fabricated cable is limited by the material PTFE as dielectric that exhibits a sharp "knee" at a temperature of 19°C [1]. To overcome this, alternative materials like PFA can be used.

The main task for the next generation of SucoPearl cables, in order to reduce even more the phase shift, is to find the appropriate combination of materials for the different cable parts InVar for the inner conductor and SiO_2 or a linear low loss polymer with opposite thermal expansion properties for the dielectric would be the best.

REFERENCES

[1] "Understanding Phase Versus Temperature Behaviour "The TeflonTM Knee", *Micro-Coax, Application Note*

[2] L.W. McKeen, "The effect of temperature and other factors on plastics and elastomers, 2nd ed.," *William Andrew, Norwich, NY, USA, 2008*

[3] S. Ebnesajjad, "Fluoroplastics, Volume 2: Melt Processible Fluoroplastics: The Definitive User's Guide", *Elsevier Science, 31.12.2002*

[4] J.J. Krempasky, "Analysis of TEM Mode on a Curved Coaxial Transmission Line," *IEEE Trans. MTT, vol. 38, No.6, pp.739-747, June 1990*